

Magazine of Civil Engineering

ISSN 2712-8172

journal homepage: http://engstroy.spbstu.ru/

Research article

UDC 691.32

DOI: 10.34910/MCE.144.3

Effects of three types of concretes on the dynamic performance of helical shell structure through finite element method

A. Hasanzadeh[1] ✉ , ***M. Hematibahar***[2] , ***N.I. Vatin***[3] , ***M. Kharun***[2]

[1] *Babol Noshirvani University of Technology, Babol, Iran*

[2] *Autonomous Non-Commercial Organization SAFAS, Razvilka, Russian Federation*

[3] *Peter the Great St. Petersburg Polytechnic University, St. Petersburg, Russian Federation*

[4] *Moscow State University of Civil Engineering (MGSU), Moscow, Russian Federation*

✉ *a_hasanzade64@yahoo.com*

Keywords: helical shell structure; dynamic performance; finite element method; time-domain history method; response spectrum method

Abstract. In this research, the dynamic performance of helical shell structure under earthquake loading is investigated using the ANSYS Workbench Finite Element software. Three different types of concretes, including high-performance concrete (HPC), basalt fiber reinforced high-performance concrete (HPC-12) and ordinary concrete (C50), were selected and the dynamic behavior of helical shell structures made by these concretes were analyzed through Response Spectrum Method (RSM) and Time History Analysis (THA), as two valuable approaches for dynamic analysis. The displacements of internal and external edges and also the displacement of the whole structure were determined by ANSYS. The results of RSM showed that C50 had the greatest internal and external displacements. The THA results indicated that C50 had the maximum displacement of external edge. However, the maximum displacement of internal edge in the structure was obtained for HPC-12. Furthermore, both types of analyses (RSM and THA) showed that for all three types of concretes, the maximum displacement of external edge of helical shell structure has been more than the internal one. It was concluded that the mechanical properties of materials considerably affect the displacement of helical shell structure.

Funding: The research was financially supported by the Ministry of Science and Higher Education of the Russian Federation within the framework of the project “Self-healing structural materials” (Agreement No. 23-28-01226 dated 04.06.2021).

Citation: Hasanzadeh, A., Hematibahar, M., Vatin, N.I., Kharun, M. Effects of three types of concretes on the dynamic performance of helical shell structure through finite element method. Magazine of Civil Engineering. 2026. 19(4). Article no. 14403. DOI: 10.34910/MCE.144.3

1. Introduction

Advanced information technology and building materials have opened up opportunities for the design of complex shell structures, particularly design of elegant thin-shell structures. Shells are able to distribute stresses uniformly over longitudinal and transverse sections. Moreover, shell structure allows engineers to design structures with larger spans requiring less building materials. As long as the design is flawless, the application of shell structure can be very delicate and efficient.

Shell structures occur widely in nature, as exemplified by soap bubbles, seashells, and bird eggs. Ancient civilizations already exploited diverse shell forms. For example, the Roman Empire was a pioneer

© Hasanzadeh, A., Hematibahar, M. Vatin, N.I., Kharun, M., 2026. Published by Peter the Great St. Petersburg Polytechnic University.

in designing domes and shell buildings [1, 2]. Such heavy stone domes required thick load-bearing walls to resist the induced stresses. However, after World War II, the rapid development of information technology changed traditional design practice. Although shell structure were already known, with the help of emerging manufacturing methods, it became possible to find and test solutions for very thin shells with large spans. Structurally, the most important advantage of shell structures is their capacity to span large distances.

The range of applications of shell structures is almost unlimited. Their use is structurally rational, economically promising, and aesthetically appealing. The shape and geometry of shells play important role in its load-bearing efficiency. If shell shape deviates from its stable geometry, the benefits of the design may be compromised. Displacements caused by various stress states can lead to irreversible deformation of the building in the worst case. Therefore, the design goal is to create a strong enough structure to withstand all possible combinations of loads associated with its performance. In [3], the response of carbon fiber reinforced polymer (CFRP) quasi-isotropic shell structures under dynamic loading was investigated. Dynamic loading was generated by shock waves in a shock-tube experimental setup. Based on the results, the mechanical behavior for quasi-isotropic CFRP under high speed, short time dynamic shock wave loads is similar to that under long time, low velocity static loads. In [4], shaking-table tests were employed to investigate the isolation performance and strong earthquake failure of a single-layer cylindrical reticulated shell structure with a lower support structure. It was found that horizontal isolation bearings can considerably reduce the horizontal seismic response of such shell, but the vertical isolation impact was poor. In [5], seismic structural performance of reinforced concrete columns strengthened by stiff-type polyuria (STPU) was studied and overall strengthening effect of the STPU for both static and dynamic loading conditions was evaluated, which can be used for retrofitting of concrete structures.

Parametric modeling proposes a flexible workflow and an efficient shell design method. This type of modeling promotes mutual understanding between architects and engineers by allowing structural optimization to be carried out in parallel with the design process. Previous studies have indicated that shells are highly effective in resisting symmetrical loads. However, structural problems arise when the shell is subjected to external asymmetrical stresses [6–10].

Recently, with the advance in technology, Finite Element Software (FES) has shown its capability to numerically simulate and model various types of structures. Moreover, different types of materials can be defined using FES [11–13]. In [14], the behavior of basalt fiber reinforced-expanded clay concrete as a building material was simulated and concluded that FES can accurately simulate the nonlinear behavior of this material. In [15], the behavior of basalt fiber reinforced high-performance concrete used in shear walls under dynamic loading was analyzed by FES. It was found that the strength of the shear wall is dependent on the mechanical characteristics of the concrete.

Despite extensive existing knowledge regarding the static behavior of shell structures, only a few studies have addressed their dynamic behavior. In [16], the performance of thin shell concrete sandwich panel was studied using FES. It was stated that thin shell structures show maximum displacement under eccentric loading. In [17], the dynamic behavior of the shear wall was investigated. High-Strength Concrete (HSC) reinforced with basalt fibers was used as the main material for the shear wall and experimental results were compared with the results obtained by FES. It was proved that FES is not only able to assess the dynamic behavior of reinforced concrete, but also can find other properties of shear walls such as hysteretic graphs. In [18], the seismic performance of a single-layer spherical reticulated shell structure was investigated. FEM was applied to a shell with a roofing system. The effects of roofing systems on the seismic performance of shells from seismic response curves, the proportions and distributions of plastic members and the failure behaviors of the shells during strong earthquakes were identified. The results indicated that the roofing system can significantly alter the seismic response and failure of a shell under strong earthquake conditions.

On the other hand, high-performance concrete (HPC) is currently a widely used material in many important structures such as highways, bridges etc., due to its suitable mechanical properties and good durability [7]. To improve the mechanical properties of HPC, fibers and additives are usually added to its mixture [19–25]. In [11], the influence of adding basalt fibers to HPC was studied. Basalt fibers were mixed with HPC at volume fractions between 0.6 % and 1.8 % (by volume of concrete), and it was concluded that the addition of 1.2 % basalt fibers had the maximum effect on the compressive and flexural strengths of HPC. In [20, 21], the effects of basalt fibers, metakaolin, and silica fume on the performance of HPC were examined. It was found that basalt fibers and metakaolin enhance the flexural and compressive strength of HPC, respectively. This research also showed that silica fume particles can effectively fill the voids between the cementitious matrix and basalt fibers.

Although there have been numerous studies on the dynamic behavior of shell structures, research on the behavior of helical shell structures under earthquake loading remains limited. Since helical shell structures are utilized in a variety of applications (such as ramps and staircases), the dynamic performance of these structures under earthquake loading is required to be investigated. Furthermore, due to the effect

of material type on the structure performance, three different types of concretes were selected including HPC, HPC with 1.2 % basalt fiber (HPC-12), and ordinary concrete (C50). The main objective of this study is to examine the dynamic behavior of helical shell structures made by these three types of concretes under earthquake loading using Time History Analysis (THA) and Response Spectrum Method (RSM).

2. Materials and Methods

2.1. Helical Shell Structure

Parametric surfaces are widely used in applied geometry and computer graphics to make complex shapes easy to process and display. When mentioning helical surfaces and their modeling, it is important to classify them based on the main shape of the materials and the axis of the helix [26]. Ruled surfaces consist of a straight line that moves in space according to the given information. The ruled surfaces are achieved by moving the generatrix along three guides and are divided into expandable and non-expandable surfaces or surfaces with zero and negative Gaussian curvature [27]. Ruled helicoids are classified depending on the rectilinear generatrix position relative to the spiral's axis and the end section. The developable helicoid is a helical surface characterized by a straight line intersecting an axis at an arbitrary angle. The Gaussian curvature is zero, where the surface curvature radius is equal to zero. Transitional motion occurs near the surface of the cylinder. In general, helical design algorithms use parametric equations as follows [10]:

$$x(u,v) = a\cos v - \frac{au\sin v}{\sqrt{a^2+b^2}}; \tag{1}$$

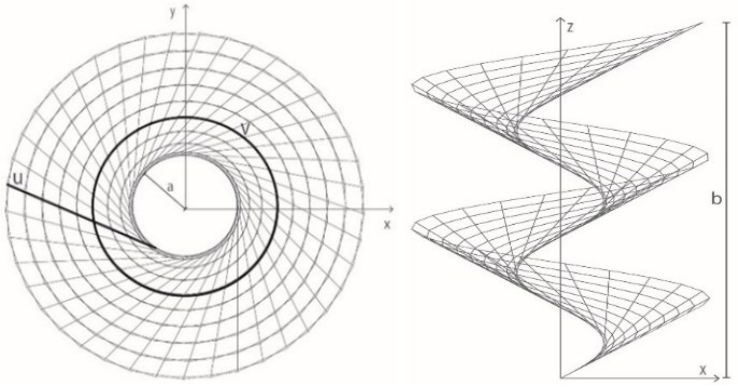
$$y(u,v) = a\sin v - \frac{au\cos v}{\sqrt{a^2+b^2}}; \tag{2}$$

$$z(u,v) = bv - \frac{bu}{\sqrt{a^2+b^2}}, \tag{3}$$

where u is the rectilinear generatrix, v is the spirals variable, a is the radius of the helicoid, b is the narrowness of the intercostal spaces of the helicoid.

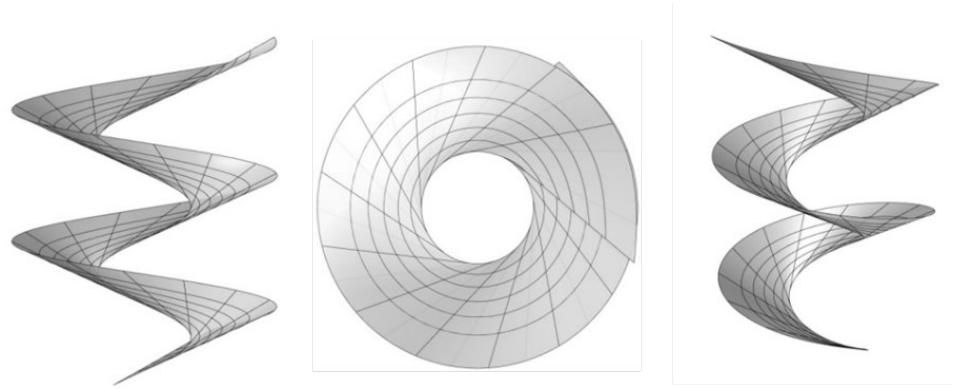
Equations (1)–(3) show that the geometry of the governing spiral surfaces is mostly mathematically analyzed and calculated [10, 28].

Parametric surfaces are usually modeled by a mixture of operators with trigonometric functions and curves. Trigonometric functions and curves are commonly used for ruled surfaces. Figs. 1 and 2 present the developable helicoid and developable helical shell structure considering (1)–(3), respectively.



a) **b)**

Figure 1. Developable helicoid: a) top view; b) side view.



a) b) c)

Figure 2. Developable helical shell structure surfaces from three sides: a) side view; b) top view; c) side view.

2.2. Methodology

In order to investigate the dynamic performance of helical shell structure under earthquake loading, ANSYS FES was employed. This software is able to simulate complex structures under different loading types through modeling materials with high accuracy [14]. In this study, at first, the geometry of helical shell structure is modeled through the Rhino 6 and Grasshopper software. The Rhino 6 software plots the surface and shell form of structure easier than other types of architectural software. Next, the geometry of helical shell structure is imported to the Geometry section of ANSYS Workbench software. It should be noted that the thickness, height and diameter of the helical shell structure were 0.4 m, 20 m and 1.5 m, respectively. The meshing size of 50 cm was selected for the structure in the modeling. The structural modeling of helical shell structure was carried out via ANSYS software and the mechanical properties of concretes (C50, HPC, HPC-12) obtained by experimental tests were assigned to the structure. According to Standard No. 2800 [29], the cumulative mass up to the modes must be larger than 80 ~ 90 % of the total mass. Moreover, in each of the two orthogonal extensions of the building, all oscillation modes that their total effective masses are more than 90 % of the total mass of the structure should be considered. Thus, six modes were taken into account in this study. The first sixth modes and natural frequencies data were obtained by the ANSYS modal analysis section. The modal analysis results were connected to the dynamic analysis section of ANSYS software. Finally, the results of dynamic analysis were analyzed by THA and RSM. Fig. 3 shows the methodology of this study.

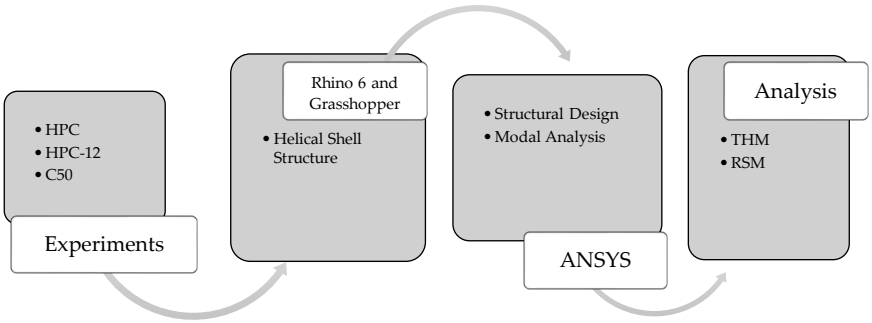


Figure 3. Methodology of the current study.

2.3. Experimental Materials

In order to use the mechanical properties of three different types of concretes including HPC, HPC-12, and C50 in the ANSYS modeling, experimental tests were initially performed on different samples. Table 1 shows the mixture design of these concretes.

Table 1. Mix proportion of concretes (kg/m^3).

Specimens	Cement	Water	Silica fume	Quartz sand	Granite	Superplasticizer	Basalt fiber
HPC	500	187.5	125	585	1005	12.5	0
HPC-12	500	187.5	125	585	1005	12.5	1.2
C50	250	157	0	771	1022	7.2	0

As seen, the following materials were utilized: ordinary Portland cement, tap water, superplasticizer, silica fume, quartz sand as fine aggregates, crushed granite as coarse aggregates and basalt fibers (1.2 % by concrete volume). The basalt fiber has been added to HPC to improve its mechanical characteristics such as compressive and tensile strengths.

A laboratory concrete pan mixer was used to blend materials at the constant rate of 48 rpm. In this regard, first, aggregates were mixed with each other for about 2 min. Then, water, cement, silica fume, and superplasticizer were added and blended. Finally, for HPC-12, fibers were manually inserted at the rate of 10 g per second and blended until a homogeneous mix was obtained. After that, a set of samples, including cylindrical samples, with diameter of 100 mm and height of 200 mm for tensile tests and cubic samples with dimensions of 100 × 100 ×100 mm for compressive tests were prepared (Fig. 4). To cure concrete specimens, they were kept under water at the temperature of approximately 20 °C. After curing for 28 days, samples were tested for determination of their compressive and tensile strength values according to GOST 10180 [30] and ASTM C496 [31], respectively. The compression and tension tests were performed using the Matest C025N machine manufactured in Mates Company, Bergamo, Italy (Fig. 5). Determination of the mechanical properties of concretes can help the reliability of the modeling in the ANSYS software.



a) **b)**

Figure 4. Types of samples: a) cubic; b) cylindrical.



Figure 5. Matest C 025N machine test.

The compressive and tensile tests were carried out at the loading rate of 600 and 200 kg/s, respectively (Figs. 6 and 7).

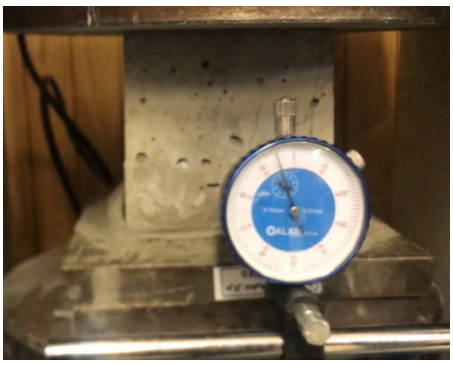


Figure 6. Compression test.

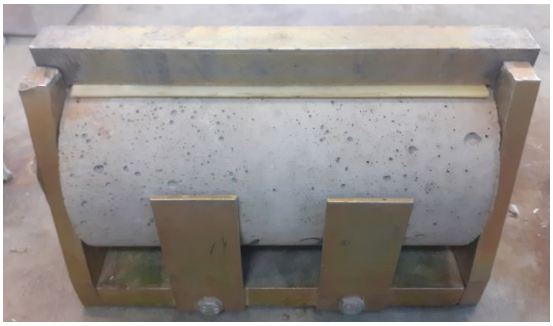


Figure 7. Tension test.

2.4. Dynamic Analysis

Seismic analysis is a subset of structural analysis which can calculate the response of a structure against lateral loads such as earthquakes. Static or linear static analysis is appropriate when effects of higher modes are not significant. This is mainly true for short buildings. However, for tall buildings or buildings with torsional irregularities, a dynamic analysis is required. The aim of dynamic analysis is to understand the behavior of structure (building) to various dynamic loads: such as wind, earthquake, machine vibration, and ambient vibration. In linear-dynamic analysis, the response of the structure to ground motion is determined in the time domain, and all phase information is therefore maintained. Indeed, in this analysis, only linear properties are assumed. The analytical method can utilize modal decomposition as a means of reducing the degrees of freedom (DOF) in the analysis. In this analysis, the building is simulated as a multi-DOF system with a linear elastic stiffness matrix and an equivalent viscous damping matrix. Moreover, the seismic input is modeled through either modal spectral analysis or THA. The advantage of linear-dynamic analysis is that it can consider higher modes.

Two types of linear-dynamic analysis methods including RSM and THA were applied in this study to evaluate the behavior of the helical shell structure under earthquake loading. It is noteworthy to mention that these methods have been presented in [32, 33], and [29]. In [34], the performance of RSM and THA taking into account these standards was studied. It was found that they are reliable for designing and analyzing the structures under seismic loading. Furthermore, it was concluded that [26] is a suitable standard for the dynamic analysis of structures. Thus, in the present study, the analysis of the helical shell structure was carried out considering this standard.

2.4.1. Response Spectrum Method (RSM)

A response spectrum is a plot of the peak or steady-state response (displacement, velocity, or acceleration) of a series of oscillators of varying natural frequencies that are forced into motion by the same base vibration or shock. RSM is a dynamic analysis method which measures the contribution from each natural mode of vibration to indicate the likely maximum seismic response of an essentially elastic structure. It estimates the structural response of short, nondeterministic, and transient dynamic events such as earthquakes and shocks. The response-spectrum analysis provides insight into dynamic behavior by measuring pseudo-spectral acceleration, velocity, or displacement as a function of the structural period for a given time history and level of damping. It is practical to envelope response spectra such that a smooth curve represents the peak response for each realization of the structural period. The RSM is performed in the following four basic steps:

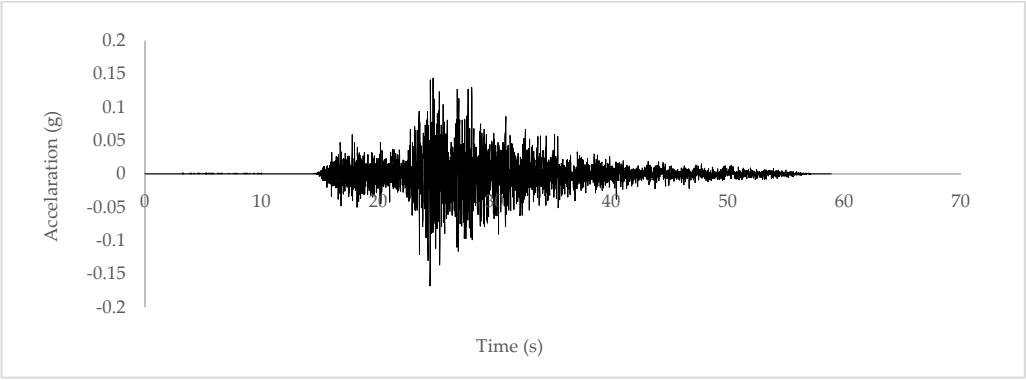
1) modal analysis of the structure;
2) calculation of the responses of the structure in each vibration mode;

3) combining the effects of the modes;

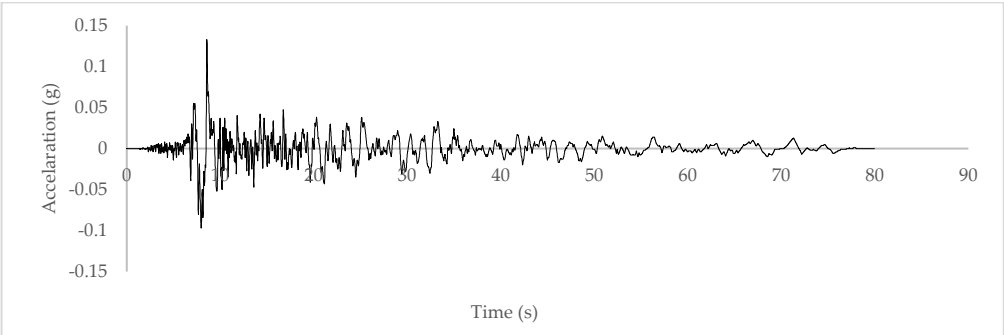
4) modifying the values of the responses of the structure.

In the modal analysis, the structural responses such as the internal forces of the members, displacement, floor shears, and support reactions are obtained separately for each mode. Due to the fact that the periods of vibration of the modes are different from each other, the maximum responses of the structure for various modes do not occur simultaneously, and, for this reason, it is not possible to determine the total response of the structure by summing the response of different modes. In spectral analysis, the final response of the structure is obtained using the superposition of its different modes (within the frequency domain). In fact, the response of the structure is a combination of various mode shapes. For each considered mode, based on the frequency and mass of the mode, the response of that mode is extracted from the design spectrum and then is combined with the response of other modes to obtain the overall response of the structure. Combination methods include Square Root Sum of Squares (SRSS) and Complete Quadratic Combination (CQC), which is a modified method of SRSS for close modes.

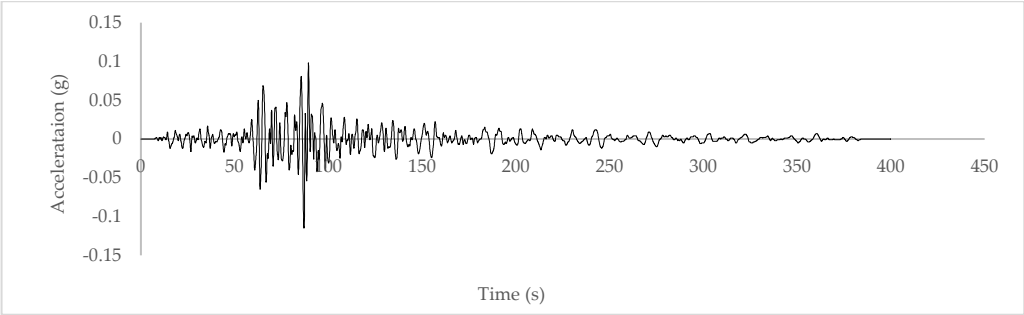
The Peak Ground Acceleration (PGA) is computed according to the factored spectral response diagram. Based on [29], at least three pairs of accelerograms belonging to the horizontal components of three different earthquakes should be selected. Thus, three different earthquake pulses including Bam, Iran (2003), Borrego Mountain, USA (1968), and Northern California, USA (1941) were selected in this research to determine the Factorized Response Spectrum (FRS) diagram. It is obvious that with increasing the number of selected records, the accuracy of the output results will be improved. FRS is called a spectrum which is scaled to the standard design spectrum with applying a coefficient factor. Fig. 8 shows the time-acceleration graphs of these earthquakes. As seen, Bam and Northern California earthquakes have the highest and lowest frequency content, respectively. Northern California earthquake has the highest period and Bam has the lowest one. Earthquake records with low and high frequency have a greater effect on tall and short structures, respectively, due to the phenomenon of resonance. Moreover, amplitude of the earthquake record is the highest in Bam earthquake. The FRS diagram is shown in Fig. 9. The SRSS and CQC are recommended to plot the FRS diagram. In this research, the SRSS used a damping ratio of 5 % of the structure weight [29, 34–37].



a)



b)



c)

Figure 8. Time-acceleration graphs for: a) Bam, Iran (2003); b) Borrego Mountain, U.S.A (1968); c) Northern California, USA (1941).

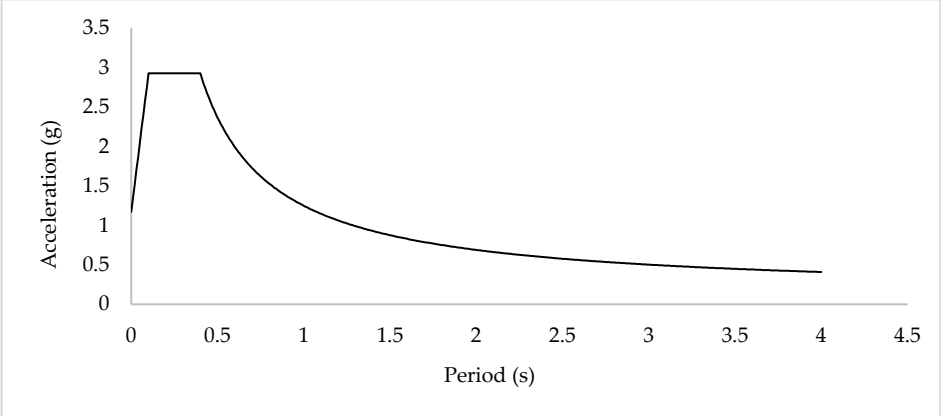


Figure 9. FRS diagram of three mentioned earthquakes.

It should be noted that any earthquake record in linear and nonlinear analyses should be scaled. Based on [29], first, each pair of records is scaled to its maximum value. Second, for the maximum value, the spectrum of the acceleration response is determined by assuming a 5 % damping ratio. The response spectra of the earthquake record are combined with each other using the SRSS method and a single spectrum is then made for each pair. Since three earthquake records were employed in this study, the maximum response spectrum value between these three records was used.

2.4.2. Time History Analysis (THA)

THA provides a correct understanding of the dynamic response of structure under seismic loading. The dynamic equilibrium equation (4) is the most important equation in the structure dynamics which is solved using either modal or direct-integration methods:

$$Ku(t)+\frac{C}{\partial t}\dot{\partial}u(t)+\frac{M}{\partial t}\ddot{\partial}u(t)=0, \tag{4}$$

where u is the displacement of the structure, K is the stiffness matrix, C is the damping matrix, t is time, M is the mass matrix.

THA is basically a method of seismic analysis for the simulation of an earthquake motion. It is a step-by-step analysis of the dynamic response of a structure to a specified loading which varies in time. In the analysis, the damping ratio was assumed to be 5 % [29] which was applied in the earthquake records during the scaling process in SeismoSignal software. The ground acceleration is determined based on the acceleration of the earthquake. Each pair of seismic records is simultaneously applied in two perpendicular directions to the structure and then the structure response is determined as a function of time.

THA for linear dynamic analysis is carried out by considering time and domain such as acceleration, frequency etc. According to [29], if less than seven accelerometers are selected for analysis, their maximum effect should be considered to control displacement and internal forces. If seven or more accelerometers are used, the average value of their effects should be taken into account. In the present research, the earthquake ground acceleration record of Bam earthquake was selected for THA (Fig. 8a). It had a 6.6 magnitude on the Richter scale with the period of less than 12 seconds [38, 39].

To perform dynamic analysis, it is important to know the DOF of the structure. It is defined as the set of independent displacements/rotations that describe the deformed shape of the structure with respect to its initial position. In other words, DOF is the number of directions that the structure can be moved freely without any restraints. For evaluation of the DOF, it is necessary to determine the supports in the structure. In this paper, the fixed-ends supports were used in the two ends of the helical structure. These supports prevent both translation and rotation in any direction. In 2D, the fixed-end support can be represented by force components parallel to the x and y axes (P_x and P_y), and a moment (M) that is perpendicular to the $x-y$ plane. Fig. 10 shows the reactions in fixed-end support. In this case, all forces and moments should be equal to zero.

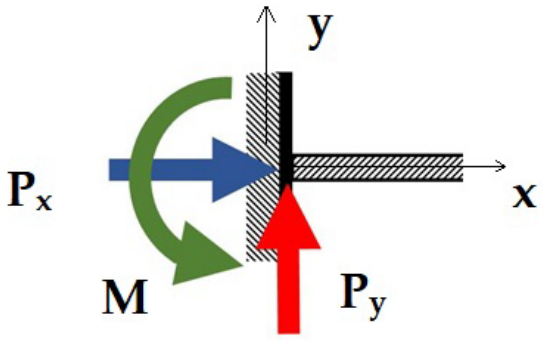


Figure 10. Fixed-end support diagram.

In this study, THA and RSM were applied to analyze the dynamic performance of helical shell structure. Besides, the total displacement of helical shell structure as well as the displacement of the internal and external edges of the helical shell structure was assessed for structures made by different concretes.

3. Results

3.1. Mechanical properties

Fig. 11 shows the stress-strain curves of samples. It can be observed that HPC-12 failed smoothly during tests, i.e., it showed the ductile behavior. This was due to the bridging effect of fibers which successfully hindered the further creation of cracks [40–43]. However, C50 and HPC failed suddenly. In other words, their failure modes were brittle. Fig. 12 shows the failure mode of samples.

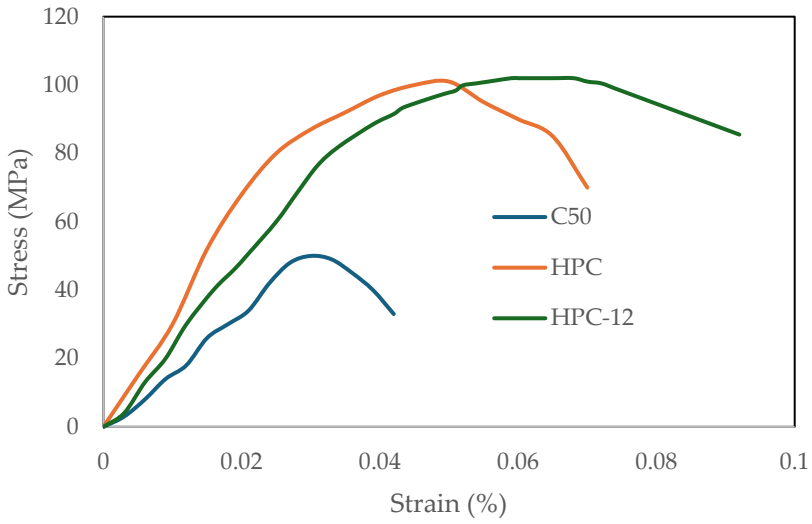


Figure 11. Stress-strain curves of the samples.



a) b) c)

Figure 12. Failure mode of the samples: a) C50; b) HPC; c) HPC-12.

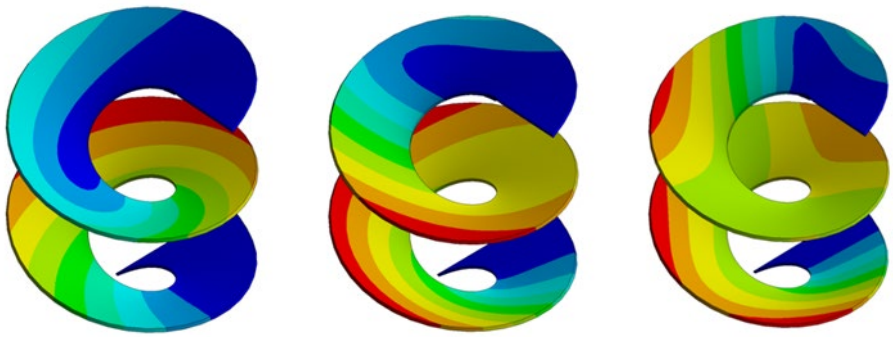
Table 2 shows the mechanical properties of concretes. As seen, HPC-12 has the maximum compressive and tensile strengths.

Table 2. Mechanical properties of different types of concretes.

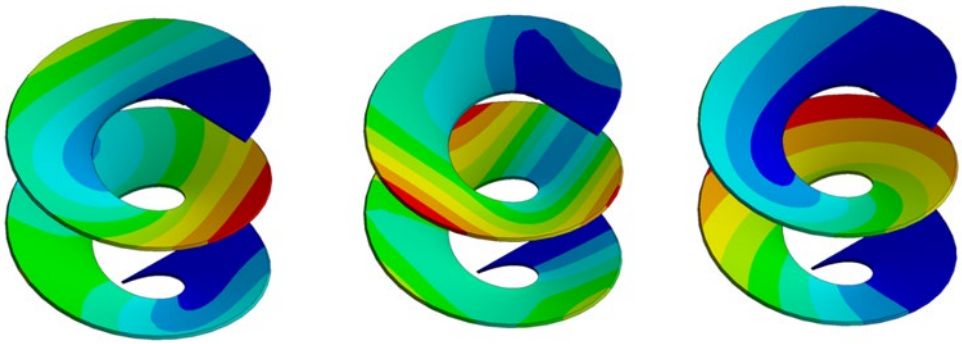
Concrete type	Compressive strength, MPa	Tensile strength, MPa	Modulus of elasticity, GPa
HPC	101.43	13.4	39.805
HPC-12	102.51	17.9	40.438
C50	50	5.68	17.600

3.2. Modal analysis

Modal analysis is a technique applied to evaluate the structure's vibration features, such as natural frequencies, mode shapes and mode participation factors (how much a given mode participates in a given direction). The deformed shape of the structure at a specific natural frequency of vibration is termed its normal mode of vibration. The natural frequencies of a structure are the frequencies at which the structure naturally tends to vibrate if it is subjected to a disturbance. Natural frequencies and mode shapes are functions of the structural characteristics and boundary conditions, and the main reasons to compute the natural frequencies and mode shapes of a structure is to determine the dynamic interaction between a component and its supporting structure. The terms "mode shape" or "natural vibration shape" are utilized in structural dynamics. A mode shape describes the displacement that the component would demonstrate when vibrating at the natural frequency. All vibration patterns have their own frequency at which they oscillate, with the lowest frequency vibration referred to as the natural mode. The first mode has the lowest frequency and highest period while the last mode has the highest frequency and lowest period. The reason for the differences between modes of the structure is that each mode has its own frequency and period and oscillates at a separate frequency from other modes; therefore, each mode has a particular response to seismic excitation. The six characteristic modal shapes were calculated by the ANSYS modal analysis section in this research. Each characteristic modal form of analysis is illustrated by a certain type of displacement in different directions. The displacement variation of each modal shape depends on the shape of the structure, thickness, and the natural frequency of that mode. Fig. 13 illustrates the six characteristic natural modal shapes for the helical shell structure. As seen, the largest structural displacement took place on the second turn, and the maximum displacement was near to the outer edge in each mode. The fixed-end supports did not demonstrate any displacement.



a) b) c)



d) e) f)

Figure 13. Displacements for modal shapes: a) 1st modal characteristic displacements; b) 2nd modal characteristic displacements; c) 3rd modal characteristic displacements; d) 4th modal characteristic displacements; e) 5th modal characteristic displacements; f) 6th modal characteristic displacements.

In the ANSYS modal section, the natural frequencies, effective mass, and modal mass participation factor were calculated for all three types of concrete. The results are presented in Table 3. The differences in these values are attributed to the different responses of each mode to the earthquake excitation. Modal mass participation ratio indicates the percentage of structural mass of the model participating in a given direction and mode.

The results of mode frequencies illustrate that the natural frequencies of HPC and HPC-12 are more than C50. Moreover, the total frequencies of the sixth mode are about five times more than the first one. The values of effective mass, mass participation factor and modal mass participation ratio did not significantly change when different concrete types were used as the structural material for the helical shell structure.

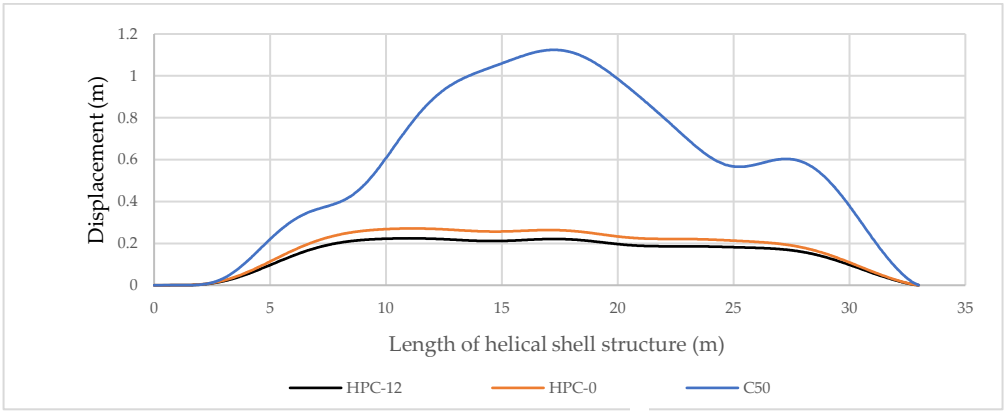
Table 3. Modal shape information for each type of concrete.

Modal No.	Frequency, Hz			Effective mass X-direction, g			Modal mass participation factor X-direction			Modal mass participation ratio X-direction		
	C50	HPC	HPC-12	C50	HPC	HPC-12	C50	HPC	HPC-12	C50	HPC	HPC-12
1	0.48725	0.7315	0.73729	6.18E+06	6.19E+06	6.19E+06	2485.5	2487.6	2487.6	0.10	0.09	0.10
2	0.52695	0.79173	0.798	4.32E+06	5.02E+06	8.03E+06	–65.629	–89.61	–89.61	0.07	0.08	0.14
3	0.81785	1.2283	1.2381	4.54E+07	4.58E+07	4.58E+07	–6739.7	–6765.4	–6765.4	0.74	0.73	0.80
4	1.1965	1.7978	1.812	2.32E+06	2.31E+06	2.31E+06	1523.2	1521	1521	0.03	0.03	0.04
5	1.5355	2.3055	2.3238	1.76E+05	1.84E+05	1.84E+05	419.88	429.02	429.02	0.002	0.002	0.003
6	2.2507	3.3827	3.4095	2.71E+06	2.70E+06	2.70E+06	–1645.6	–1642.6	–1642.6	0.04	0.04	0.04

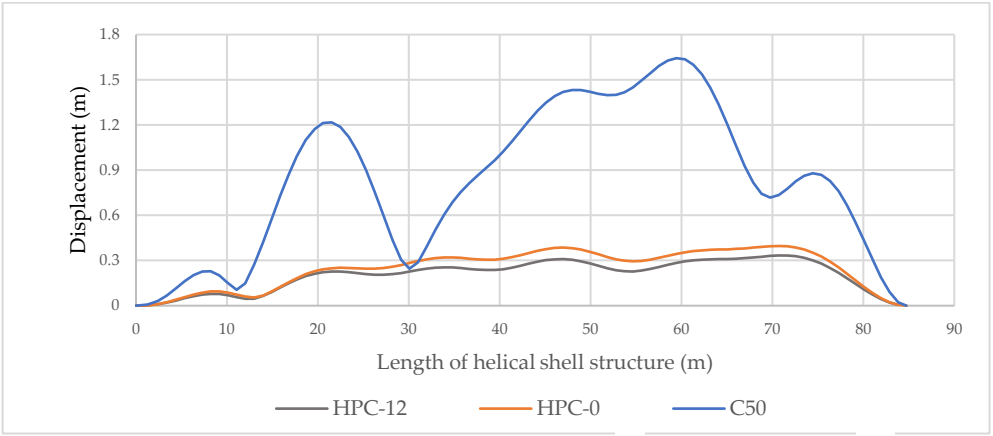
3.3. RSM

According to the RSM results, the maximum displacement of C50, HPC-12, and HPC has been 47, 32, and 42 cm, respectively. Thus, the maximum displacement of the structure occurs when C50 is used. The displacement of the structure has a strong relationship with earthquake acceleration and mechanical properties of concrete such as compressive and tensile strengths.

Fig. 14 shows the obtained displacements of internal and external edges of helical shell structure. As observed, for all types of concretes, the displacement of external edge has been more than the internal one. Moreover, C50 demonstrated more internal and external displacements comparing HPC-12 and HPC.



a)



b)

Figure 14. Displacement of edges: a) internal edge; b) external edge.

Based on the analysis, the maximum displacement for the external and internal edges has been 1.64 and 1.12 m, respectively (for C50). Besides, the maximum displacements of the external and internal edges occur on the second and first turn, respectively.

3.4. THA

The Bam earthquake was the basis of THA in this study. Fig. 15 shows the total displacement of the helical shell structure under earthquake loading. As seen, the first and second turns of the helical shell structures are the critical zones. In fact, the critical zones have the highest potential for the development of cracks and failure in the structure because they show the maximum displacement under earthquake loading. The maximum displacement for HPC-12, HPC and C50 has been approximately 18, 21 and 23 cm, respectively. Thus, C50 is an inappropriate material to be used in helical shell structures among others.

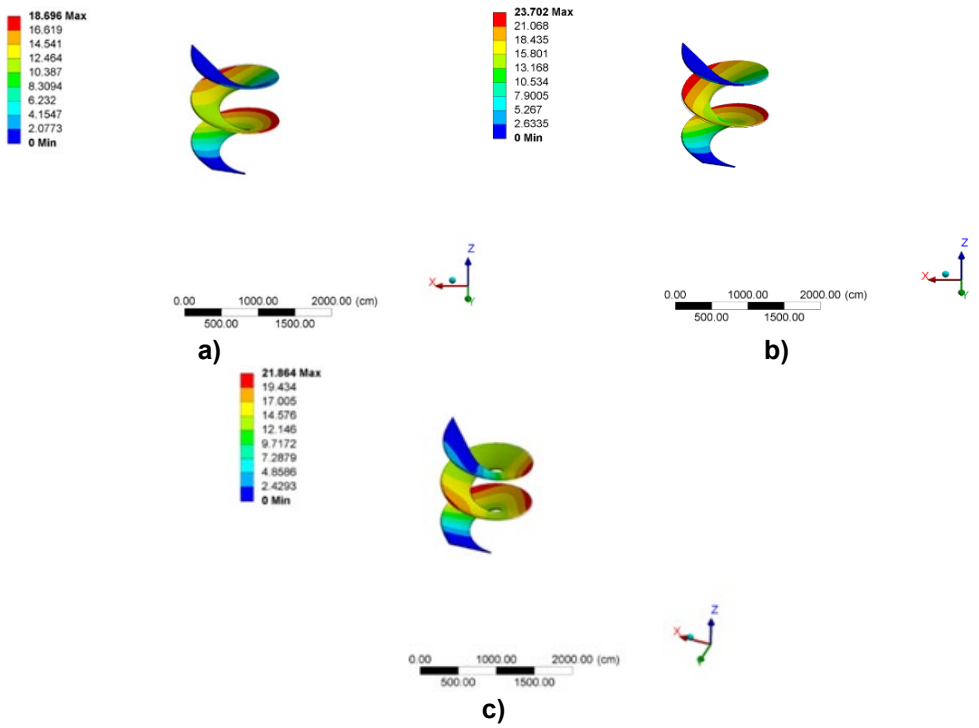
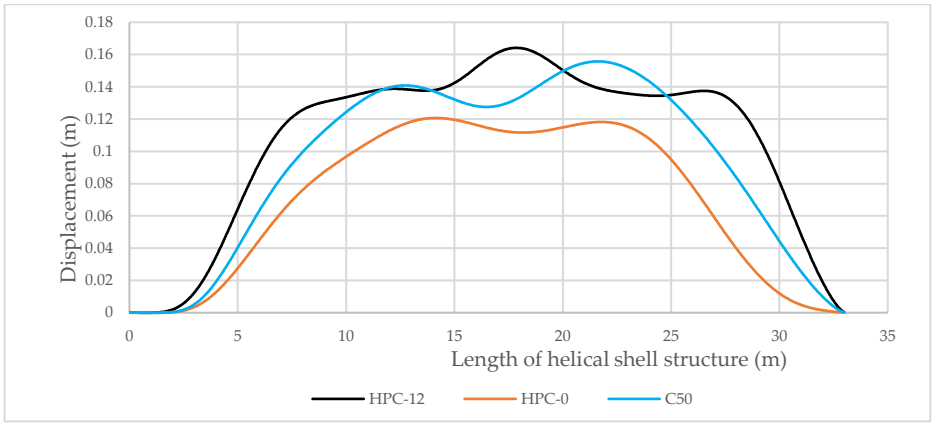
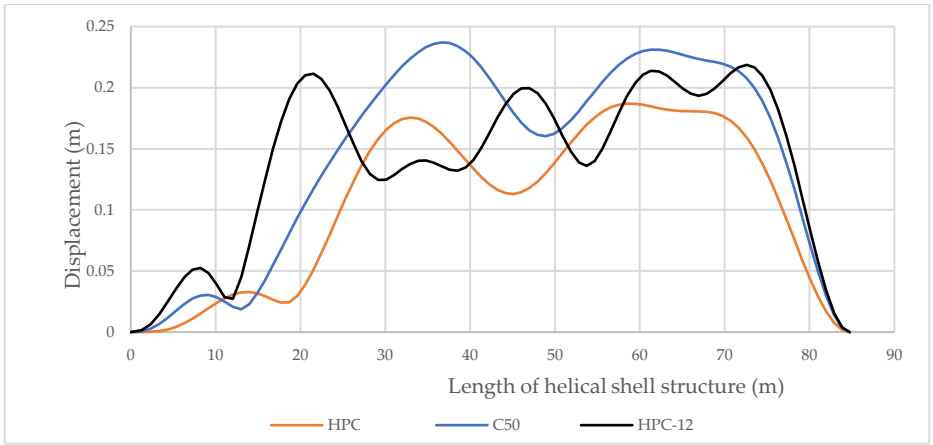


Figure 15. Total displacement (cm) for different types of concretes: a) HPC-12; b) C50; c) HPC.

Fig. 16 indicates the displacement of internal and external edges. As seen, the maximum displacement of external edges has been more than the internal ones. Moreover, C50 had the maximum displacement of external edge among other types of concretes. The maximum displacement of internal edge was obtained when HPC-12 was used.



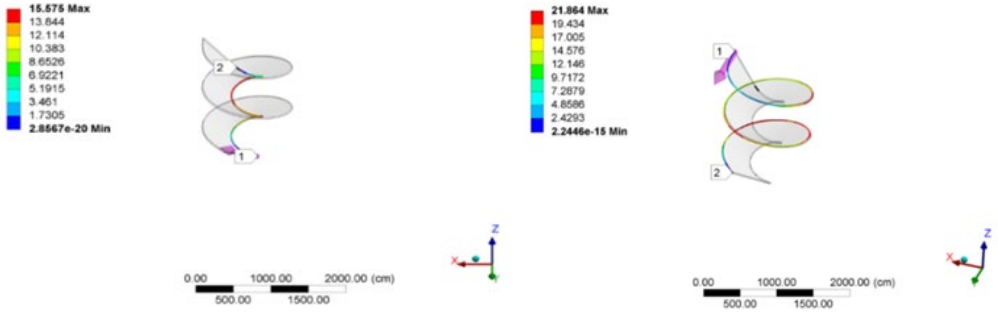
a)



b)

Figure 16. Displacement of edges: a) internal edge; b) external edge.

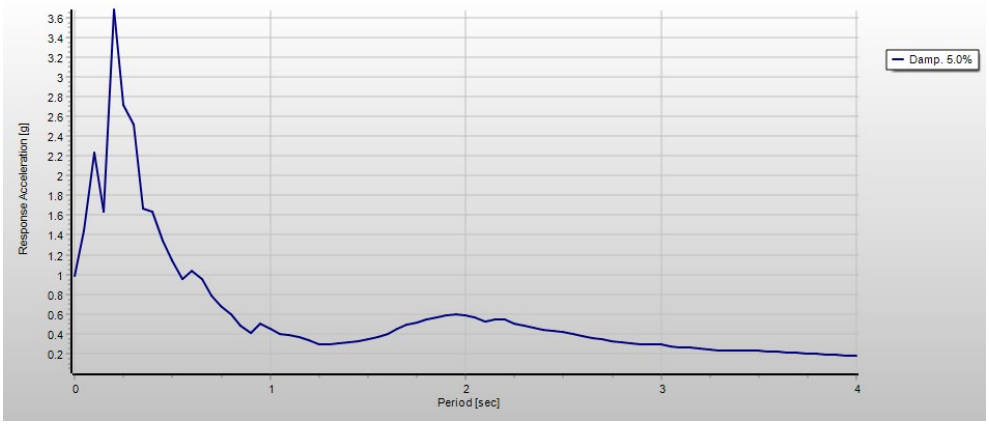
Fig. 17 shows the external and internal displacements of helical shell structure when C50 is used. The external edge showed more displacement than the internal one. Besides, the maximum displacement of internal edge was on the second turn while for the external edge, the maximum displacement occurred between the first and second turns. Therefore, C50 is considered as the unsuitable material to be used in helical shell structure because of its weak mechanical properties.



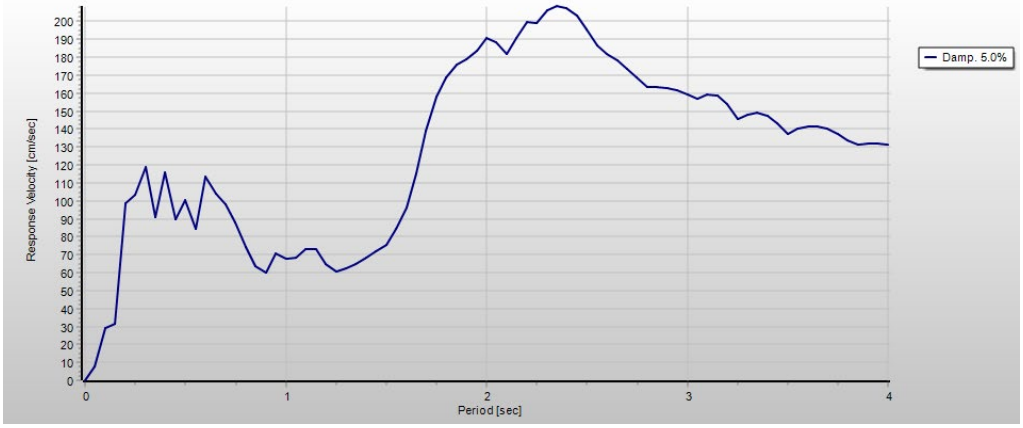
a) **b)**

Figure 17. Displacement (cm) of (a) internal and (b) external edge for C50.

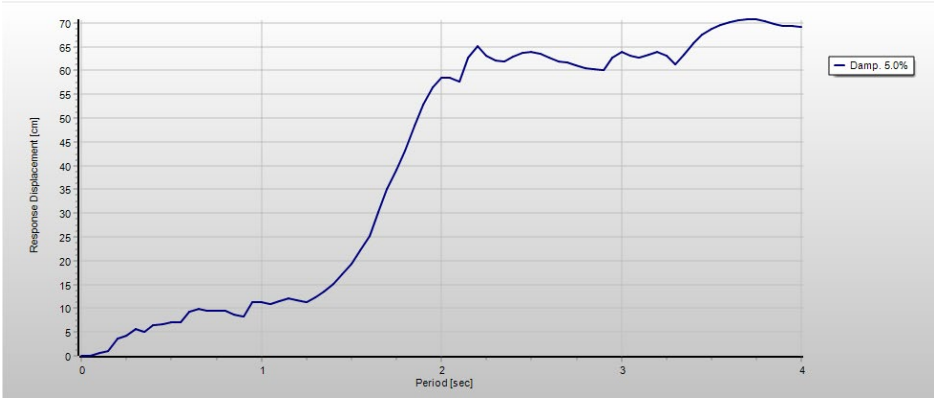
When examining the results of a dynamic analysis, one can refer to the response spectra such as acceleration, velocity and displacement spectra. Response spectra are very useful tools for analyzing the performance of structures and equipment in earthquakes. The displacement, velocity, and acceleration response spectra are defined as the maximum values caused by the acceleration history. Fig. 18 indicates the response spectra which were obtained through SeismoSignal software considering Bam earthquake record. It should be noted that all these spectra were achieved regarding 5 % damping as mentioned earlier.



a)



b)



c)

Figure 18. Response spectra: a) acceleration; b) velocity; c) displacement.

3.5. Period Analysis

As presented in Table 3, the frequency increases with increasing modal number. The period of each mode can be calculated through the mode frequency. In fact, the period has an inverse relationship with the frequency:

$$f = \frac{1}{T}, \tag{5}$$

where f and T are frequency and period, respectively. Therefore, the period decreases with increasing the modal number. This result is shown in Fig. 19.

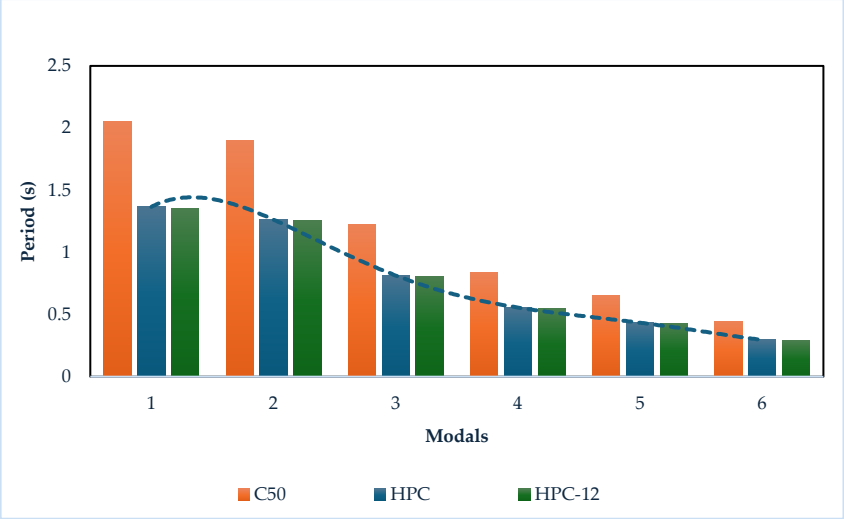


Figure 19. Values of periods in all modes.

3.6. Validation

For validation, the natural frequencies of the helical shell were compared with the analytical and numerical results in [44], where the behavior of the helical reinforced concrete columns subjected to horizontal 2D seismic motion excitation was studied. In his research, the seismic behavior of the helical reinforced concrete columns under a seismic load of the short period was investigated using ANSYS FES. The comparison of frequencies (modal analysis results) for structures made with ordinary concrete in both studies illustrated that there is an appropriate agreement between the results (Fig. 20).

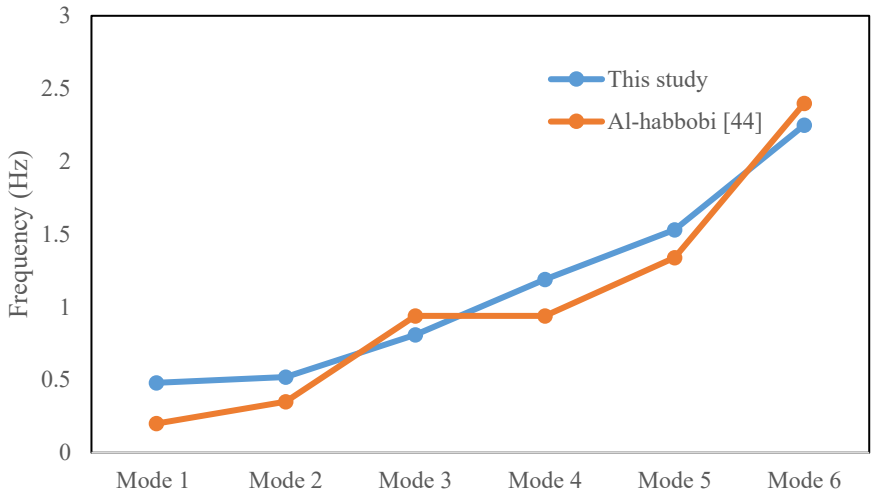


Figure 20. Comparison of the results.

Table 4 presents the comparison between the first three natural frequencies of the helical shell obtained in the present FE model and those reported in [44]. The maximum deviation is less than 3 %, which confirms the accuracy of the present modeling approach.

Table 4. Mode numbers of validation for this study.

Mode No.	Present study frequency, Hz	[44] frequency, Hz	Difference, %
1	3.27	3.35	2.4%
2	5.91	6.02	1.8%
3	8.44	8.60	1.9%

A mesh sensitivity analysis was also performed in order to ensure the independence of the results from the element size. Three mesh densities were investigated, ranging from 15000 to 58000 elements. As shown in Table 5, the variation of the first natural frequency becomes less than 1 % once the mesh reaches 58000 elements. Therefore, the fine mesh (≈58000 elements) was adopted for all nonlinear dynamic analyses.

Table 5. Mesh sensitivity.

Mesh type	Number of elements	First mode frequency, Hz	Difference, %
Coarse	15000	3.19	2.1%
Medium	32000	3.24	1.6%
Fine	58000	3.27	0.9%

4. Discussion

The results showed that C50 had the maximum displacement in the external edge among other types of concretes due to its lower tensile and compressive strengths. However, the HPC-12 illustrated the maximum displacement in the internal edge. Thus, it can be stated that the external edge of helical shell structure was more influenced using concrete with low mechanical properties. However, the internal edge of the helical shell structure was more affected using concrete with high mechanical properties. In [45], the behavior of helical shell structure made by basalt fiber reinforced lightweight concrete was investigated via SCAD FES. It was confirmed that the external edge of the helical shell structure has the maximum displacement when concrete with low mechanical properties is used while the internal edge of this structure experienced the maximum displacement when concrete with high mechanical properties is utilized. These results are compatible with the results of the present research. It was also reported that stronger material had less displacement under loading. It should be noted that, in this study, the ANSYS was employed which

has better performance than SCAD. For example, ANSYS is able to demonstrate the displacement of different sections of helical shell structure.

In the THA, the highest internal edge displacement was obtained for the HPC-12, which appears counter-intuitive considering the higher compressive strength and stiffness of this material. This behavior can be explained by the dynamic characteristics of the helical shell. Increasing the elastic modulus of concrete reduces the global period of the structure, which shifts the dominant vibration modes toward higher frequencies. For the Bam earthquake record, the predominant frequency content lies within a range that becomes closer to the modal frequencies of the HPC-12 configuration. As a result, despite its higher stiffness, the structure experiences a larger dynamic amplification under THA. Moreover, the reduced density of HPC-12 slightly decreases the mass participation in the fundamental modes. In THA, lower mass leads to larger accelerations being transmitted into the structure, which in turn intensifies local deformations in regions of high modal curvature, such as the inner helix edge. This effect is more pronounced in helical shells, whose geometry produces mixed bending and torsion mode shapes with significant localization of deformation.

These combined effects – frequency shifting due to stiffness, increased acceleration demand due to reduced mass, and the complex modal interaction inherent to helical geometries – explain why the HPC-12 configuration produced the largest internal edge displacement in THA, even though it exhibited superior mechanical strength. Since the modal mass participation ratios remain nearly unchanged for all three concrete types (Table 3), the higher internal edge displacement in HPC-12 cannot be attributed to differences in modal mass participation. Instead, it is mainly governed by the stiffness-induced shift in modal frequencies, which brings the dominant modes of the HPC-12 configuration closer to the predominant frequency content of the Bam earthquake record. Furthermore, the inner edge of the helical shell exhibits higher curvature and localized bending and torsion coupling. These regions are more sensitive to higher-frequency modal components, which become more pronounced in stiffer materials such as HPC-12. As a result, the internal edge undergoes larger localized amplification under THA even though the stiffness of HPC-12 is higher.

Based on the obtained results, THA was more reliable than the RSM in terms of analysis. These findings are in agreement with the results of [46], where the shell structure using FES was analized and it was found that the dynamic behavior of the shell structure depends on its shape, loading and material type. It was concluded that RSM analysis is also able to find the displacement of different types of shell structures. Nevertheless, THA revealed more reasonable results than RSM.

5. Conclusions

In this research, ANSYS FES was applied to investigate the dynamic performance of helical shell structure under earthquake loading. For this purpose, three types of concretes (HPC, HPC-12, and C50) and two methods of dynamic analyses (RSM and THA) were used. The external and internal edges of the helical shell structure showed different structural behavior using different types of concretes. Based on the calculated outcomes, the following conclusion is obtained:

1. The results of RSM showed that C50 demonstrated more internal and external displacements comparing to HPC-12 and HPC, when used in the helical shell structure.
2. The results of THA indicated that C50 had the maximum displacement of external edge among other types of concrete. However, the maximum displacement of internal edge in the structure was obtained for HPC-12.
3. Both types of analyses (RSM and THA) showed that the maximum displacement of external edges has been more than the internal ones in the helical shell structure.
4. It can be stated that stiffer structures have higher natural frequencies for the same boundary conditions. Furthermore, the mechanical properties of concrete significantly affect the displacement of the helical shell structure.

References

1. Boyer, C.B. A History of Mathematics. NY, London, Sydney: JohnWiley & Sons, Inc., 1968.
2. Masi, F., Stefanou, I., Vannucci, P. On the origin of the cracks in the dome of the pantheon in Rome. Engineering Failure Analysis. 2018. 92. Pp. 587–596. DOI: 10.1016/j.engfailanal.2018.06.013
3. Khawaja, H.A., Bertelsen, T.A., Andreassen, R., Moatamedi, M. Study of CRFP shell structures under dynamic loading in shock tube setup. Journal of Structures. 2014. Article no. 487809. DOI: 10.1155/2014/487809
4. Liang, N., Zhi, X., Nie, G., Fan, F. Experiment and analysis of seismically isolated single-layer cylindrical reticulated shell structure. Journal of Structural Engineering. 2022. 148(4). Article no. 04022009. DOI: 10.1061/(ASCE)ST.1943-541X.0003262

5. Lee, T.-H., Choi, S.-J., Yang, D.-H., Jay Kim, J.-H. Experimental seismic structural performance evaluations of RC columns strengthened by stiff-type polyurea. International Journal of Concrete Structures and Materials. 2022. 16. Article no. 65. DOI: 10.1186/s40069-022-00552-6
6. Hejazi, M., Pourabedin, M. Performance of Persian brick masonry discontinuous double-shell domes against earthquakes. Engineering Failure Analysis. 2021. 119. Article no. 104994. DOI: 10.1016/j.engfailanal.2020.104994
7. Cohen, J.W. On stress calculations in helicoidal shells and propeller blades. TNO Ship & Navigation. 1955. Report no. 215.
8. Rynkovskaya, M. Analytical methods of analysis of right and open helicoids. American Society for Engineering Education Northeast Section Conference. Advanced Structured Materials 2009. Pp. 157–171. DOI: 10.1007/978-3-319-79005-3_11
9. Iaroshenko, A.R. Osesimmetrichnaia deformatsiia vintovoi obolochki s priamougol'nym profilem [Axisymmetric deformation of a helical shell with a rectangular profile]. Dinamika i prochnost' mashin [Dynamics and Strength of Machines]. 1971. 12. Pp. 3–9.
10. Krivoshapko, S., Rynkovskaya, M. Five types of ruled helical surfaces for helical conveyers, support anchors and screws. MATEC Web of Conference (ICMME 2016). 2017. 95. Article no. 06002. DOI: 10.1051/matecconf/20179506002
11. Hematibahar, M. Crack Resistance in Basalt Fibred High-Performance Concrete. Master's Thesis, Department Civil Engineering, People Friendship University of Russia (RUDN), Moscow, Russia, 2021.
12. Lam, T.V., Vu, D.T., Dien, V.K., Bulgakov, B.I., Korol, E.A. Properties and thermal insulation performance of lightweight concrete. Magazine of Civil Engineering. 2018. 84(8). Pp.173–191. DOI: 10.18720/MCE.84.17
13. Stolarski, T., Yoshimoto, S., Nakasone, Y. Engineering Analysis with ANSYS Software, 2nd ed. London: Butterworth-Heinemann, 2018. DOI: 10.1016/C2016-0-01966-6
14. Galishnikova, V.V., Kharun, M., Koroteev, D.D, Chiadighikaobi, P.C. Basalt fiber reinforced expanded clay concrete for building structures. Magazine of Civil Engineering. 2021. 101(1). Article no. 10107. DOI: 10.34910/MCE.101.7
15. Kharun, M., Koroteev, D.D., Hemati Bahar, M., Huang, J., Kamrunnaher, M. Behavior of conventional and fibered concrete shear walls during earthquake, an analytical simulation in SAP2000. Journal of Physics: Conference Series. 2020. 1678. Article no. 012033. DOI: 10.1088/1742-6596/1687/1/012033
16. Alchaar, A., Abed, F. Finite element analysis of a thin-shell concrete sandwich panel under eccentric loading. Journal of Building Engineering. 2020. 32. Article no. 101804. DOI: 10.1016/j.jobe.2020.101804
17. Li, X., Zhang, J., Cao, W. Hysteretic behavior of high-strength concrete shear walls with high-strength steel bars: experimental study and modelling. Engineering Structures. 2020. 214. Article no. 110600. DOI: 10.1016/j.engstruct.2020.110600
18. Li, W., Zhi, X., Fan, F. Influence of the roofing system on the seismic performance of single-layer spherical reticulated shell structures. Buildings. 2022. 12(2). Article no. 155. DOI: 10.3390/buildings12020155
19. Kosmatka, S.H., Wilson, M.L. Design and Control of Concrete Mixtures: The guide to applications, methods and materials, 5th ed. Skokie, Illinois (USA): Portland Cement Association, 2011.
20. Ayub, T., Shafiq, N., Nuruddin, M.F. Mechanical properties of high-performance concrete reinforced with basalt fibers. Procedia Engineering. 2014. 77. Pp. 131–139. DOI: 10.1016/j.proeng.2014.07.029
21. Ayub, T., Shafiq, N., Nuruddin, M.F. Effect of chopped basalt fibers on the mechanical properties and microstructure of high performance fiber reinforced concrete. Advances in Materials Science and Engineering. 2014. Article no. 587686. DOI: 10.1155/2014/587686
22. Kharun, M., Koroteev, D. Effect of basalt fibres on the parameters of fracture mechanics of MB modifier based high-strength concrete. MATEC Web of Conferences. 2018. 251. Article no. 02003. DOI: 10.1051/matecconf/201825102003
23. Hematibahar, M., Milani, A., Fediuk, R., Amran, M., Bakhtiary, A., Kharun, M., Mousavi, M.S. Optimization of 3D-printed reinforced concrete beams with four types of reinforced patterns and different distances. Engineering Failure Analysis. 2025. 168. 109096. DOI: 10.1016/j.engfailanal.2024.109096
24. Momeni, K., Vatin, N.I., Hematibahar, M., Gebre, T.H. Repair overlays of modified polymer mortar containing glass powder and composite fibers-reinforced slag: mechanical properties, energy absorption, and adhesion to substrate concrete. Frontiers in Built Environment. 2024. 10. Article no. 1479849. DOI: 10.3389/fbuil.2024.1479849
25. Momeni, K., Vatin, N.I., Hematibahar, M., Gebre, T.H. Differences between 3D printed concrete and 3D printing reinforced concrete technologies: a review. Frontiers in Built Environment. 2025. 10. Article no. 1450628. DOI: 10.3389/fbuil.2024.1450628
26. Krivoshapko, S.N., Ivanov, V.N. Encyclopedia of Analytical Surfaces. Cham: Springer, 2015. DOI: 10.1007/978-3-319-11773-7
27. Flöry, S., Pottmann, H. Ruled Surfaces for Rationalization and Design in Architecture. LIFE in:formation. On Responsive Information and Variations in Architecture. 2010. Pp. 103–109.
28. Krivoshapko, S.N., Ivanov, V.N. Analiticheskie metody rascheta obolochek nekanonicheskoi formy [Analytical methods for the analysis of shells of non-canonical shape]. Moscow: RUDN, 2010.
29. Building and Housing Research Center. Iranian Code of Practice for Seismic Resistant Design of Buildings. IRSt2800. 2014
30. Nauchno-issledovatel'skii, proektno-konstruktorskii i tekhnologicheskii institut betona i zhelezobetona (NIIZHB). Concretes. Methods for strength determination using reference specimens. GOST 10180. 2012. 32 p.
31. Advancing Standards Transforming Markets International (ASTM International). Standard Test Method for Splitting Tensile Strength of Cylindrical Concrete Specimens. ASTM C496-96. 2017. 4 p. DOI: 10.1520/C0496-96
32. American Society of Civil Engineering (ASCE). Seismic Rehabilitation of Existing Buildings. ASCE/SEI 41-06. 2007. 411 p. DOI: 10.1061/9780784408841
33. American Society of Civil Engineering (ASCE). Seismic Evaluation and Retrofit of Existing Buildings. ASCE/SEI 41-13. 2014. DOI: 10.1061/9780784416112
34. Harati, M., Hojjati, A., Modaraei, A. An investigation on the effect of the near-fault earthquakes on the seismic behavior of RC moment resisting frames (MRFs) designed based on Iranian Seismic Code (Standard No. 2800). arXiv:1907.03234. 2019. DOI: 10.48550/arXiv.1907.03234
35. Augusti, G. Dynamics of structures: theory and applications to earthquake engineering. Meccanica. 1996. 31. Pp. 719–720. DOI: 10.1007/BF00426980
36. Zhao, M., Gao, Z., Wang, P., Du, X. Response spectrum method for seismic analysis of monopile offshore wind turbine. Soil Dynamics and Earthquake Engineering. 2020. 136. Article no. 106212. DOI: 10.1016/j.soildyn.2020.106212

37. Jhung, M.J., Choi, Y., Oh, C.-S. Earthquake response of a core shroud for APR1400. Nuclear Engineering and Technology. 2021. 53 (8). Pp. 2716–2727. DOI: 10.1016/j.net.2021.02.007
38. Maleki-Asayesh, B., Zafarani, H., Tatar, M. Coulomb stress changes and secondary stress triggering during the 2003 (Mw 6.6) Bam (Iran) earthquake. Tectonophysics. 2020. 775. Article no. 228304. DOI: 10.1016/j.tecto.2019.228304
39. Rezaei, S., Moradi, M., Hasanzadeh, A. Numerical investigation of the parameters influencing site effects. Journal of Civil Engineering Researchers. 2025. 7. Pp. 10–20. DOI: 10.61186/JCER.7.2.10
40. Hasanzadeh, A., Shooshpasha, I. A study on the combined effects of silica fume particles and polyethylene terephthalate fibres on the mechanical and microstructural characteristics of cemented sand. International Journal of Geosynthetics and Ground Engineering. 2021. 7. Article no. 98. DOI: 10.1007/s40891-021-00340-4
41. Hasanzadeh, A., Shooshpasha, I. Influences of silica fume particles and polyethylene terephthalate fibers on the mechanical characteristics of cement-treated sandy soil using ultrasonic pulse velocity. Bulletin of Engineering Geology and the Environment. 2022. 81. Article no. 14. DOI: 10.1007/s10064-021-02494-x
42. Hasanzadeh, A., Shooshpasha, I. Influence of PET fibres on the tensile characteristics of cemented sand treated with silica fume. Road Materials and Pavement Design. 2025. 26 (5). Pp. 1041–1064. DOI: 10.1080/14680629.2024.2399251
43. Hasanzadeh, A., Shooshpasha, I. PET fiber reinforcement efficiency in the mechanical and microstructural characteristics of cemented sand modified with silica fume. Construction and Building Materials. 2023. 397. Article no. 132363. DOI: 10.1016/j.conbuildmat.2023.132363
44. Al-habbobi, A.M. Numerical analyses on seismic behavior of helical concrete columns. IOP Conference Series: Materials Science and Engineering. 2019. 584. Article no. 012007. DOI: 10.1088/1757-899X/584/1/012007
45. Chiadighikaobi, P.C., Jean Paul, V., Brown, C.K.S. The effectiveness of basalt fiber in lightweight expanded clay to improve the strength of concrete helicoidal staircase. Materials Science Forum. 2021. 1034. Pp. 187–192. DOI: 10.4028/www.scientific.net/MSF.1034.187
46. Ding, L.R. Integrating form-finding of brick shell structure into the design of new architecture in seism-affected Groningen. Master's Thesis. Delft University of Technology (TU Delft), Delft, The Netherlands, 2016.

Information about the authors:

***Ali Hasanzaden**, PhD*
ORCID: https://orcid.org/0000-0001-5546-0950
E-mail: a_hasanzade64@yahoo.com

***Mohammad Hematibahar**,*
ORCID: https://orcid.org/0000-0002-0090-5745
E-mail: eng.m.hematibahar1994@gmail.com

***Nikolai Vatin**, Doctor of Technical Sciences*
ORCID: https://orcid.org/0000-0002-1196-8004
E-mail: vatin@mail.ru

***Makhmud Kharun**, PhD in Technical Sciences*
ORCID: https://orcid.org/0000-0002-2773-4114
E-mail: miharun@yandex.ru

Received: 18.09.2023. Approved: 13.06.2026. Accepted: 14.06.2026.